Check for updates

Nonlinear vortex beam array generation by spatially modulated fundamental wave

HUI LI,[1,2] **HAIGANG LIU,**[1,2] **AND XIANFENG CHEN**[1,2,*]

[1]*State Key Laboratory of Advanced Optical Communication Systems and Networks, School of Physics and Astronomy, Shanghai Jiao Tong University, Shanghai 200240, China*
[2]*Key Laboratory for Laser Plasma (Ministry of Education), Collaborative Innovation Center of IFSA (CICIFSA), Shanghai Jiao Tong University, Shanghai 200240, China*
[*]*xfchen@sjtu.edu.cn*

Abstract: We experimentally demonstrated the generation of a dynamic nonlinear vortex beam array by utilizing a fundamental wave with a modulated phase structure, which was incident into a homogeneous nonlinear medium. In our experiment, one-dimensional and two-dimensional second harmonic vortex beam arrays were investigated, and the topological charge of second harmonic vortex beam of different order was measured. This study presents a method of dynamic control of the nonlinear vortex beam array, which may have applications in multiple-particles optical trapping, optical communication, and so on.

OCIS codes: (190.0190) Nonlinear optics; (050.1970) Diffractive optics; (190.2620) Harmonic generation and mixing; (080.4865) Optical vortices.

References and links

1. A. T. O'Neil, I. MacVicar, L. Allen, and M. J. Padgett, "Intrinsic and extrinsic nature of the orbital angular momentum of a light beam," Phys. Rev. Lett. **88**(5), 053601 (2002).
2. R. A. Beth, "Mechanical detection and measurement of the angular momentum of light," Phys. Rev. **50**(2), 115–125 (1936).
3. L. Allen, M. W. Beijersbergen, R. J. C. Spreeuw, and J. P. Woerdman, "Orbital angular momentum of light and the transformation of Laguerre-Gaussian laser modes," Phys. Rev. A **45**(11), 8185–8189 (1992).
4. D. G. Grier, "A revolution in optical manipulation," Nature **424**(6950), 810–816 (2003).
5. M. F. Andersen, C. Ryu, P. Cladé, V. Natarajan, A. Vaziri, K. Helmerson, and W. D. Phillips, "Quantized rotation of atoms from photons with orbital angular momentum," Phys. Rev. Lett. **97**(17), 170406 (2006).
6. M. Padgett and R. Bowman, "Tweezers with a twist," Nat. Photonics **5**(6), 343–348 (2011).
7. J. E. Curtis and D. G. Grier, "Structure of optical vortices," Phys. Rev. Lett. **90**(13), 133901 (2003).
8. Z. Shen, L. Su, X. C. Yuan, and Y. C. Shen, "Trapping and rotating of a metallic particle trimer with optical vortex," Appl. Phys. Lett. **109**(24), 241901 (2016).
9. A. Mair, A. Vaziri, G. Weihs, and A. Zeilinger, "Entanglement of the orbital angular momentum states of photons," Nature **412**(6844), 313–316 (2001).
10. J. Wang, J. Y. Yang, I. M. Fazal, N. Ahmed, Y. Yan, H. Huang, Y. Ren, Y. Yue, S. Dolinar, M. Tur, and A. E. Willner, "Terabit free-space data transmission employing orbital angular momentum multiplexing," Nat. Photonics **6**(7), 488–496 (2012).
11. N. V. Bloch, K. Shemer, A. Shapira, R. Shiloh, I. Juwiler, and A. Arie, "Twisting light by nonlinear photonic crystals," Phys. Rev. Lett. **108**(23), 233902 (2012).
12. G. H. Shao, Z. J. Wu, J. H. Chen, F. Xu, and Y. Q. Lu, "Nonlinear frequency conversion of fields with orbital angular momentum using quasi-phase-matching," Phys. Rev. A **88**(6), 063827 (2013).
13. K. Shemer, N. Voloch-Bloch, A. Shapira, A. Libster, I. Juwiler, and A. Arie, "Azimuthal and radial shaping of vortex beams generated in twisted nonlinear photonic crystals," Opt. Lett. **38**(24), 5470–5473 (2013).
14. S. M. Li, L. J. Kong, Z. C. Ren, Y. Nan Li, C. H. Tu, and H. T. Wang, "Managing orbital angular momentum in second-harmonic generation," Phys. Rev. A **88**(3), 035801 (2013).
15. F. Kong, C. Zhang, F. Bouchard, Z. Li, G. G. Brown, D. H. Ko, T. J. Hammond, L. Arissian, R. W. Boyd, E. Karimi, and P. B. Corkum, "Controlling the orbital angular momentum of high harmonic vortices," Nat. Commun. **8**(14970), 14970 (2017).
16. G. Gariepy, J. Leach, K. T. Kim, T. J. Hammond, E. Frumker, R. W. Boyd, and P. B. Corkum, "Creating high-harmonic beams with controlled orbital angular momentum," Phys. Rev. Lett. **113**(15), 153901 (2014).
17. D. Gauthier, P. R. Ribič, G. Adhikary, A. Camper, C. Chappuis, R. Cucini, L. F. DiMauro, G. Dovillaire, F. Frassetto, R. Géneaux, P. Miotti, L. Poletto, B. Ressel, C. Spezzani, M. Stupar, T. Ruchon, and G. De Ninno, "Tunable orbital angular momentum in high-harmonic generation," Nat. Commun. **8**(14971), 14971 (2017).
18. A. Shapira, A. Libster, Y. Lilach, and A. Arie, "Functional facets for nonlinear crystals," Opt. Commun. **300**, 244–248 (2013).

19. S. Lightman, R. Gvishi, G. Hurvitz, and A. Arie, "Shaping of light beams by 3D direct laser writing on facets of nonlinear crystals," Opt. Lett. **40**(19), 4460–4463 (2015).
20. A. Libster-Hershko, S. Trajtenberg-Mills, and A. Arie, "Dynamic control of light beams in second harmonic generation," Opt. Lett. **40**(9), 1944–1947 (2015).
21. B. K. Singh, R. Remez, Y. Tsur, and A. Arie, "Super-Airy beam: self-accelerating beam with intensified main lobe," Opt. Lett. **40**(20), 4703–4706 (2015).
22. R. Ni, Y. F. Niu, L. Du, X. P. Hu, Y. Zhang, and S. N. Zhu, "Topological charge transfer in frequency doubling of fractional orbital angular momentum state," Appl. Phys. Lett. **109**(15), 151103 (2016).
23. B. Yang, X. H. Hong, R. E. Lu, Y. Y. Yue, C. Zhang, Y. Q. Qin, and Y. Y. Zhu, "2D wave-front shaping in optical superlattices using nonlinear volume holography," Opt. Lett. **41**(13), 2927–2929 (2016).
24. H. Liu, J. Li, X. Zhao, Y. Zheng, and X. Chen, "Nonlinear Raman-Nath second harmonic generation with structured fundamental wave," Opt. Express **24**(14), 15666–15671 (2016).
25. V. Denisenko, V. Shvedov, A. S. Desyatnikov, D. N. Neshev, W. Krolikowski, A. Volyar, M. Soskin, and Y. S. Kivshar, "Determination of topological charges of polychromatic optical vortices," Opt. Express **17**(26), 23374–23379 (2009).
26. V. G. Shvedov, C. Hnatovsky, W. Krolikowski, and A. V. Rode, "Efficient beam converter for the generation of high-power femtosecond vortices," Opt. Lett. **35**(15), 2660–2662 (2010).
27. M. V. Berry, "Optical vortices evolving from helicoidal integer and fractional phase steps," J. Opt. A, Pure Appl. Opt. **6**(2), 259–268 (2004).

1. Introduction

It is well known that optical angular momentum is composed of spin angular momentum and orbital angular momentum (OAM) [1]. The OAM of light was firstly observed in 1930s [2]. In 1992, Allen et al. verified that OAM has an azimuthal phase term $e^{il\varphi}$, where l and φ represent the topological charge and azimuth angle, respectively [3]. In the last two decades, optical OAM has attracted great interest due to its potential applications in various research fields, such as optical trapping [4–8], quantum computation [9], optical communications [10]. In the field of optical trapping, the beam carrying OAM can be used to rotate particles with different angular velocities [4–8]. Quantum computation and quantum imaging have been realized by utilizing the entanglement of optical OAM [9]. In addition, such optical OAM could also be used to increase the capacity of optical communications [10]. The nonlinear generation process enables vortex beams to be obtained at new wavelengths, which opens up new possibilities for all-optical switching and manipulation of vortex beams. Hence, second harmonic generation (SHG) [11–14], sum-frequency generation [11–13], difference frequency generation [12] and even high-harmonic [15–17] of the vortex beam has been investigated. To get SHG of the vortex beam, there are two main methods. One is to manipulate the structure of nonlinear photonic crystals (NPCs) [11,13]. The other is to pattern the output facet of a nonlinear crystal [18,19], which combines both the nonlinear process and the beam spatial shaping. However, these two methods possess the same drawbacks, including complex fabrication and unchangeable nonlinear wave patterns. To solve these problems, some researchers turn their attention to pre-shaping the fundamental wave (FW) before its incidence into a nonlinear crystal [14,20–23]. In our previous researches, we have already introduced the structured FW into nonlinear frequency conversion processes. For example, the nonlinear Raman-Nath SHG of different types of FW was achieved [24].

In this paper, we experimentally demonstrated the nonlinear vortex beam array dynamically generated by utilizing the FW with a modulated phase structure via a spatial light modulator (SLM), which was incident into a homogeneous nonlinear medium. In the one-dimensional (1D) case, a series of second harmonic (SH) vortex beam was achieved in 1D direction. In the two-dimensional (2D) case, SH vortex beam array in 2D direction was generated. Besides, the topological charge of SH vortex beam of different order located in such SH vortex beam array was also experimentally measured.

2. Theoretical analysis

The phase structure of the FW was periodically and sharply modulated from 0 to ϕ into fork-shaped structure. The diffraction of FW is negligible in case of long-period modulation

of the FW in a sufficient short medium [24]. And supposing the light propagates along the y-axis (longitudinal direction) of the crystal, in 1D case, the FW is given in the form of the Fourier series by:

$$E_1 = A_1 \exp\left[-i\left(k_1 y - \omega t\right)\right] \cdot \sum C_m \exp\left[-i2\pi m f\left(\vec{r}, \varphi\right) - i m l_1 \varphi\right], \qquad (1)$$

where A_1 and k_1 are the amplitude and wave vector of the FW, respectively. C_m is the Fourier coefficients ($C_0 = \left(1 + e^{i\phi}\right)/2$, $C_{m \neq 0} = \dfrac{i\left[\cos\left(m\pi\right) - 1\right]}{2m\pi}\left(1 - e^{i\phi}\right)$).
$\vec{r} = x\vec{x} + y\vec{y}$, $\varphi = \tan^{-1}\left(z/x\right)$ is the azimuthal angle, $f\left(\vec{r}, \varphi\right) = \left|\vec{r}\right|\cos\left(\varphi\right)/\Lambda$ is the spiral structure function, Λ is spatial period of the plane wave, l_1 is the topological charge of the FW. The SH can be expressed as $E_2 = A_2 \exp\left[-i\left(\vec{k}_{2t} \cdot \vec{r} + k_{2y} y - 2\omega t\right)\right]$, where A_2 , $\vec{k}_{2t}$ and k_{2y} represent the amplitude, transverse and longitudinal wavevector, respectively. Under the non-depletion assumption, the evolution of the SH wave can be written as [15]:

$$\frac{dA_2}{dy} = \varepsilon_0 \chi^{(2)} A_1^2 \cdot \sum b_u \exp\left(ik_{2y} y - i2k_1 y\right) \cdot \exp\left[i\vec{k}_{2t} \cdot \vec{r} - i2\pi u f\left(\vec{r}, \varphi\right)\right] \cdot \exp\left(iul_1 \varphi\right), (2)$$

where $b_u = \sum_{m,n}^{m+n=u} C_m C_n$ is the Fourier coefficient of the nonlinear polarization. In Eq. (2), the first exponential term denotes the longitudinal phase mismatch, the middle exponential term is the nonlinear Raman-Nath diffraction, and the last exponential term represents the topological charge of the generated SH vortex beam. As can be seen, the topological charge of the generated SH vortex beam obeys the law of $l_{SH} = ul_1$.

When the phase is modulated in 2D, the FW can be expressed as

$$E_1 = A_1 e^{-i\left(k_1 y - \omega t\right)} \cdot \sum_{m=-\infty}^{m=+\infty} C_m e^{-im\left[2\pi f_1\left(\vec{r}, \varphi\right) + l_x \varphi\right]} \cdot \sum_{p=-\infty}^{p=+\infty} C_p e^{-ip\left[2\pi f_2\left(\vec{r}, \varphi\right) + l_z \varphi\right]}, \qquad (4)$$

where l_x and l_z are the topological charges of the FW along x and z direction, respectively. Then the coupled wave equation of SH can be written as:

$$\frac{dA_2}{dy} = \varepsilon_0 \chi^{(2)} A_1^2 \cdot e^{i\left(k_{2y} - 2k_1\right)y} \sum_{u=-\infty}^{u=+\infty} b_u \sum_{v=-\infty}^{v=+\infty} b_v e^{i\left[\vec{k}_{2t} \cdot \vec{r} - 2\pi u f_1\left(\vec{r}, \varphi\right) - 2\pi v f_2\left(\vec{r}, \varphi\right)\right]} \cdot e^{i\left(ul_x + vl_z\right)\varphi}, \quad (5)$$

where $b_u = \sum_{m,n}^{m+n=u} C_m C_n$ and $b_v = \sum_{p,q}^{p+q=v} C_p C_q$. In this case, the topological charge of the SH vortex beam is $l_{SH} = ul_x + vl_z$.

3. Experimental results and discussion

In our experiments, a Nd:YAG nanosecond laser with a wavelength and a repetition rate of 1064 nm and 20 Hz, respectively, was applied. The sample was a homogenous 5-mol% MgO:LiNbO$_3$ crystal ($10 \times 0.5 \times 10$ mm^3 in x × y × z dimensions). The FW was an ordinary wave and incident into the crystal along the y direction. The nonlinear process was Type-I (oo-e) phase matching. The FW was modulated by a SLM, whose resolution is 512×512 pixels and each with a square area of $19.5 \times 19.5 \, \mu m^2$. A 4-f system was used to imprint the phase structure on the nonlinear crystal and the beam waist was 2 mm. A shortpass filter was placed after the crystal to obstruct the FW. At last, the generated SH vortex beam array was projected on a screen and then recorded by a camera.
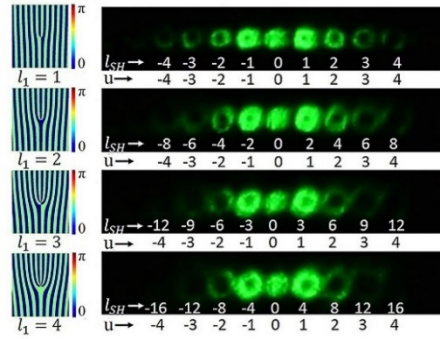
Fig. 1. Left column: The different phase structures of the FW with 0-π/2 phase modulation. Right column: The generated SH vortex beams in different orders of nonlinear Raman-Nath diffraction. $l_{SH} = ul_1$ for the uth order SH.

In order to illuminate the relationship between the generated SH vortex beam array and the structure of the FW, we firstly imprinted different fork-shaped structured FW in 1D case onto the nonlinear crystal. The structure of the FW is shown in the left column of Fig. 1, where the fork-shaped phase structure is 0-π/2 sharply modulated. The duty cycle is 0.5. The corresponding experimental results of the SH vortex beams are shown in the right column of Fig. 1, where u represents the Raman-Nath order. The phase singularity (dark core) always exists as long as l_{SH} is nonzero. The radius of the SH vortex ring gets larger as the topological charge increases. According to Eq. (2), the topological charge of the SH vortex beam obeys the law of $l_{SH} = ul_1$ for the uth order SH. In order to determine the topological charge of the vortex beam in different orders, we measured it by utilizing a cylindrical lens [25,26]. The results are displayed in Fig. 2, which corresponds to the $l_{SH} = \pm 1, \pm 2, \pm 3$ orders of the SH vortex beam in the case of $l_1 = 1$. The number of dark stripes equals to the topological charge of the SH, which agrees well with the theoretical prediction.

$l_{SH} = -3$ $\quad$ $l_{SH} = -2$ $\quad$ $l_{SH} = -1$ $\quad$ $l_{SH} = 1$ $\quad$ $l_{SH} = 2$ $\quad$ $l_{SH} = 3$
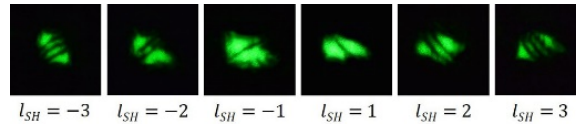
Fig. 2. The measurement of the topological charge by a cylindrical lens when $l_{SH} = \pm 1, \pm 2, \pm 3$. The number of the dark stripes represents the topological charge.
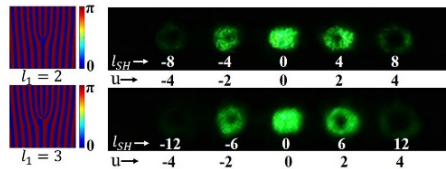

Fig. 3. Left column: different phase structures of the FW with 0-π phase modulation. Right column: The generated SH vortex beam in different orders of nonlinear Raman-Nath diffraction. $l_{SH} = ul_1$ for the uth order SH.

When the FW phase was sharply modulated from 0 to π, the odd orders of SH vortex beam vanishes, as shown in Fig. 3. Because the Fourier coefficients C_m are zero when m is even, as a result $b_u = 0$ ($b_u = \sum_{m,n}^{m+n=u} C_m C_n$) if u is odd.

In addition to the generation of SH vortex beam with integer topological charges, the case of fraction topological charge was also investigated. The FW structure is shown in the left column of Fig. 4 and the corresponding experimental results are shown in the right column. It is interesting that the SH vortex beam was not a closed ring when l_{SH} was not an integer. In this case, a dark stripe exists on the SH vortex beam according to Berry's theory in 2004 [27]. As the topological charge of the SH vortex beam was further tuned away from the integer, the gap becomes larger. For example, the gap is the largest when l_{SH} is a half-integer ($l_{SH} = 2.5$). When l_{SH} is close to an integer (such as $l_{SH} = 2.9$ shown the $+1$ order in the right column of the last row of Fig. 4), the SH vortex beam returned to a ring. Similar to the integer cases of SH vortex beam ($l_{SH} \neq 0$), the phase singularity still exists and the radius of the ring is determined by the topological charge l_{SH}.
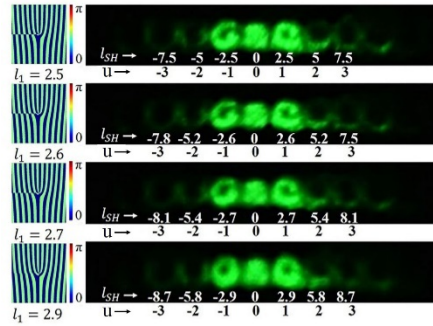

Fig. 4. Left column: Different phase structures of the FW with 0-π/2 phase modulation with fractional topological charge $l_1 = 2.5, 2.6, 2.7, 2.9$, respectively. Right column: The generated SH vortex beams in different orders of nonlinear Raman-Nath diffraction. $l_{SH} = ul_1$ for the uth order SH.

Figure 5 shows the process after the vortex beams passing through the cylindrical lens with the topological charge changing from 2 to 3. The original two dark stripes correspond to $l_{SH} = 2$. With the fractional topological charge of SH vortex beams increasing, another dark stripe comes into being and becomes more and more obvious. At last, the right bright stripe splits into two stripes completely when l_{SH} is close to 3.
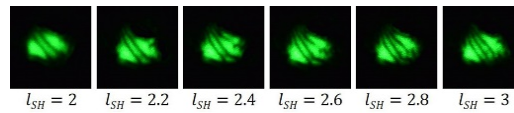

Fig. 5. Evolution of dark stripes with the topological charge changing from 2 to 3.

To further reveal the flexibility of our method, the 2D SH vortex beam array generation was studied. The structure of the FW is modulated along the x and z direction, as shown in the top row of Fig. 6, where l_x and l_z denote the topological charge of the fork-shaped FW along the x-axis and z-axis, respectively. The 2D SH vortex beam array was achieved, as shown in the bottom row of Fig. 6. The topological charge of the SH vortex beam located in the SH vortex beam array can be written as $l_{SH} = ul_x + vl_z$, where ul_x and vl_z are the topological charge along x and z-axis, respectively. The topological charges of SH vortex beams of different orders are measured to be identical to the analysis ($l_{SH} = ul_x + vl_z$).
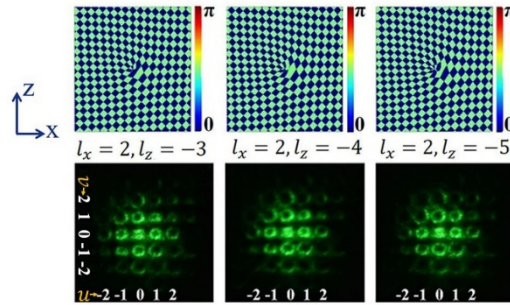
Fig. 6. Top row: The different phase structures of the FW with 0-π/2 phase modulation. l_x and l_z represent the topological charge along x and z axis, respectively. Bottom row: The generated SH vortex beams in different orders of nonlinear Raman-Nath diffraction. $l_{SH} = ul_x + vl_z$ for the (uth, vth) order SH.

Compared with the method of modulating NPCs, our method is much more convenient, since it is dynamically controlled. Different from [14] where the authors conducted the experiment making use of diffraction of FW, we paid much attention to the nonlinear diffraction process. In ref [14], two FWs with different topological charge were incident into the nonlinear crystal. In our experiment, the whole phase structure of the FW loaded on the SLM was printed onto the nonlinear crystal. Hence, the completely different experimental phenomena were obtained. SH vortex array in 1D and 2D cases are also systematically studied in our work.

4. Conclusion

In summary, we experimentally demonstrated the nonlinear vortex beam array dynamically generated by utilizing the FW, in a homogeneous nonlinear medium. In 1D cases, the topological charge obeys the law of $l_{SH} = ul_1$ in different orders. In 2D case, SH vortex beam array in 2D direction can be generated and the topological charge obeys the law of $l_{SH} = ul_x + vl_z$. Besides, the topological charge of SH vortex beam of different orders located in such SH vortex beam array was also experimentally measured. This study presents a method of dynamic control of the nonlinear vortex beam array, which may have applications in multiple-particles optical trapping, optical communication, and so on.

Funding